Int. J. Heat Mass Transfer. Vol. 36, No. 4, pp. 887–897, 1993
Printed in Great Britain

0017-9310/93 $6.00 + 0.00

Steam distillation of a single component hydrocarbon liquid in porous media

ZENG-GUANG YUAN and KENT S. UDELL†
Department of Mechanical Engineering, University of California at Berkeley, Berkeley, CA 94720, U.S.A.

(*Received* 13 *November* 1991 *and in final form* 12 *May* 1992)

Abstract—Steam distillation of a single component hydrocarbon liquid in a one-dimensional porous medium of infinite domain was studied both theoretically and experimentally. Theory was developed to describe the spatial distributions of the hydrocarbon concentration in the vapor phase, and of the liquid hydrocarbon and water saturations. A similarity solution was obtained for the case of a single component hydrocarbon where the steam quality and injection rate were constant. The characteristic velocity of the distillation zone was found to depend on the residual saturation of the hydrocarbon liquid, and the thermodynamic properties of water and the hydrocarbon liquid. The scaling between the lengths of the mass transfer zone and the variable water saturation region was characterized by appropriate dimensionless parameters. In addition to verifying the analytical predictions, experimental results allowed the determination of the mass transfer coefficient which was found to increase linearly with the saturation of the liquid hydrocarbon.

INTRODUCTION

STEAM distillation of hydrocarbon mixtures in porous media plays an important role in a number engineering applications, such as steam-flooding of oil reservoirs, which has been proven to be an effective thermal method of enhanced oil recovery in both heavy oil and light oil reservoirs [1–6]. Results of recent theoretical studies, laboratory investigations, and field practices also show great potential for steam displacement in the decontamination of underground aquifers [7–9].

A great effort has been made to understand the underlying physical mechanisms which lead to high oil recovery by steam-flooding. In the early 1960s, Willman *et al.* [10] performed a series of tests and concluded that the principal mechanisms responsible for the high oil recovery by steam displacement are (1) thermal expansion of the oil, (2) viscosity reduction and (3) steam distillation. In a critical review of steam-flood mechanisms, Wu [11] gave a detailed description of steam distillation and considered it as one of the most important mechanisms for oil recovery by steam. Blevins *et al.* [6] studied the results of light-oil steam-flood laboratory tests, computer simulations, and field projects and concluded that distillation would dominate if steam were injected into light-oil reservoirs. Based on a new theoretical model and experimental results, Stewart and Udell [12] pointed out that high recoveries by steam-flooding result partially from enhanced mass transfer from the residual oil to the steam. They also explained that two different phenomena included in the distillation are thermodynamically controlled vaporization of volatile components during a hot waterflood and mass-transfer-limited evaporation in the steam region. In their later work [9], the mass transfer processes during steam displacement were explained in more detail. Low boiling point liquids are mobilized by the process of alternating vaporization and condensation taking place in a limited region ahead of and progressing along with the steam condensation front. As a result of the removal of light components from the oil, the liquid phase concentrations and thus the vapor pressures of the remaining 'semi-' and 'non-volatile' components in the liquid oil increase, which leads to an increase in the evaporation rates of heavy end components in the steam zone.

Many laboratory studies have been conducted to quantify the yields of steam distillation. Farouq Ali [13] estimated that 5–10% of the heavy oil recovery and as much as 60% of the light oil recovery may be attributed to steam distillation. Johnson *et al.* [14] showed that the oil recovery by distillation ranges from 54.7 to 94.0% of the immobile oil volume. Wu and Brown's [15] results indicated that the distillation yields of six crude oils with gravities ranging from 1.0 to 0.84 g cm^{-3} [9–36° API] were from 7 to 57% of the steam-contacted oil. Based on their tests on 16 crude oils, Wu and Elder [16] obtained distillation yields ranging from 13 to 57% of the initial oil volume at a steam distillation factor (V_w/V_o) of 20. Duerksen and Hsueh [17] developed correlations of steam distillation yields vs other properties of oils obtained from experiments on 10 crude oils taking into account variations of pressure and temperature. All this experimental work provided useful information on the amount of distillable oil. However, the results were obtained for various durations of steam injection and steam flow rates, and thus are difficult to generalize. No detailed

† Author to whom all correspondence should be addressed.

NOMENCLATURE

c	mass concentration of the compound in the vapor phase
c_s	saturated mass concentration of the compound in the vapor
c_{pr}	specific heat of the solid phase of the porous matrix
c_{pw}	specific heat of the water
e	internal energy
f_1	fractional flow function
f_2	$k_{rv} \cdot f_1$
g	gravitational acceleration
g_m	mass transfer coefficient
g_{md}	dimensionless mass transfer coefficient, g_m/g_{rf}
g_{rf}	reference mass transfer coefficient
h	enthalpy
h_{sw}	latent heat of water
h_{vl}	latent heat of the compound
$J(s_w)$	dimensionless capillary
k	permeability
k_{rv}	relative permeability of the vapor phase
k_{rw}	relative permeability of the water phase
m_{in}	total injected mass flux of steam and condensed water
m_v	mass flux of the vapor mixture
m_w	mass flux of water phase
N_{gr}	gravity number (defined in the text)
N_{mf}	dimensionless mass transfer number (defined in the text)
p_c	capillary pressure
p_v	pressure of the vapor mixture
p_w	pressure of the water phase
s	saturation
t	time variable
T_f	temperature at the steam condensation front
T_i	initial temperature far ahead of the steam condensation front
V_l	cumulative production of liquid compound
V_w	cumulative production of water
v_c	characteristic velocity of the distillation zone
v_{cd}	dimensionless characteristic velocity of the distillation zone
v_f	velocity of the steam condensation front
v_{fd}	dimensionless velocity of the steam condensation front
v_v	velocity of vapor
v_{vd}	dimensionless velocity of vapor
x	space coordinate
X	injected steam quality.

Greek symbols

α	angle of the flow relative to horizontal
η	space coordinate in the moving coordinate system
μ	viscosity
ξ	dimensionless space coordinate in the moving coordinate system
ρ	density
σ_{vw}	interfacial tension between the vapor mixture and water phase
ϕ	porosity of the medium.

Subscripts

l	liquid compound
s	steam
v	vapor mixture
w	water
∞	far downstream
$-\infty$	far upstream.

discussion of the distillation process has been reported.

Currently, predictions of steam distillation rates in thermally enhanced oil recovery operations are obtained from numerical simulators. In all steamflood simulators, equilibrium between the liquid phase and the vapor phase oil is assumed at each node point. However, it takes time (and thus transversed distance) for the vapor to reach equilibrium with the liquid phase oil remaining in the steam zone. Unfortunately, this time (and length) scale is not currently known. Therefore there is a need for a more rigorous analysis of the mechanics of steam distillation of hydrocarbon liquids, particularly regarding the issues of (1) mass transfer-controlled evaporation; (2) relationships between the spatial distribution of the liquid hydrocarbon saturation and its vapor concentration given the mass transfer and the thermodynamic equilibrium constraints; and (3) the coupling of steam condensation and the energy requirement for the hydrocarbon evaporation process.

The objective of the present work is to provide an analytic model of the steam distillation of single component hydrocarbon liquid and then identify the features of the controlling processes in the removal of liquid hydrocarbon compounds from porous media. In order to evaluate the applicability of the model, comparisons are made between theoretical and experimental results.

FORMULATION OF A SINGLE COMPONENT DISTILLATION MODEL

Figure 1 is a schematic of steam distillation of a single component hydrocarbon liquid in a one-dimensional porous medium initially saturated with water

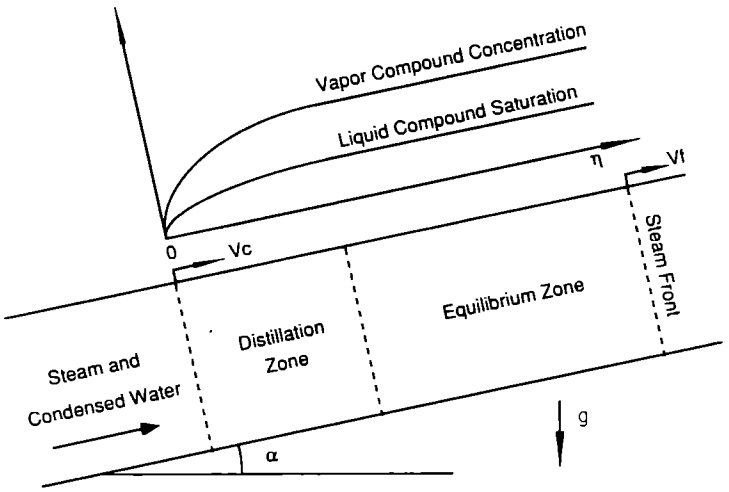

FIG. 1. Steam distillation of a single component hydrocarbons in a one-dimensional porous solid.

and a hydrocarbon liquid. Steam is injected far upstream at a constant mass flux. For adiabatic conditions and relatively high permeability, the steam moves through the porous medium and condenses at the steam front which advances with a constant velocity v_f [12, 18]. The region behind the steam condensation front is referred to as the steam zone. This steam zone consists of three subregions: a zone nearest the steam injection face where only steam and condensed water exist, a distillation zone, and an equilibrium zone. We define the interface between the distillation zone and the zone where only water exists as the distillation front. The distillation front propagates downstream with a velocity v_c. Downstream from the distillation front, within the distillation zone, the liquid hydrocarbon evaporates and becomes dispersed as a gas within the flowing steam; here there are three coexisting fluid phases: the vapor phase consisting of steam and hydrocarbon, the condensed water phase, and the liquid hydrocarbon phase. Evaporation of the liquid hydrocarbon occurs until, at a point far enough downstream, the vapor phase becomes saturated with the hydrocarbon and equilibrium is reached. This point marks the interface between the distillation zone and the equilibrium zone. The equilibrium zone extends from the distillation zone to the steam front. In this study it is assumed that the steam and condensed water, the distillation, and the equilibrium zones are all present within the steam zone.

Before the steam condensation front arrives, the porous medium experiences a long period of waterflooding, first at the initial temperature, and then at elevated temperatures as the condensation front approaches. In addition, the large gas phase pressure gradients present at the steam front [12, 18] provide even greater liquid mobilization forces. Therefore, it is reasonable to assume that for many cases of interest, the saturation of liquid hydrocarbon in the steam zone is at or below the immobile residual level whereas the vapor and the liquid phases of water are flowing.

The recovery of the hydrocarbon liquid from the steam zone is limited by its rate of vaporization occurring within the distillation zone. The rate of vaporization is in turn affected by the velocity of the distillation front, the equilibrium concentration of the hydrocarbon vapor in the gas phase, the mass of hydrocarbon per unit volume in the equilibrium zone, and the mass flux of steam. The length of the distillation zone depends on the mass transfer coefficient between the flowing gas and the hydrocarbon liquid: for a small mass transfer coefficient, the distillation zone length will be large, whereas a large mass transfer coefficient ensures that the steam becomes fully saturated with the hydrocarbon vapor within a short distance from first contact with the hydrocarbon liquid.

The steam zone as the modelling region

We assume that the flow in the porous medium is one-dimensional and that the length of the distillation zone is much less than that of the porous medium. Thus, far upstream, the mass flow rates for water and steam are assumed given, and far downstream in the equilibrium zone, the vapor mixture is saturated with the hydrcarbon. In between exists the distillation zone, where there is continuous evaporation of the liquid hydrocarbon. As such, the saturation of the liquid hydrocarbon will decrease with time until the hydrocarbon is completely removed. The distillation zone can therefore be idealized as moving downstream in an infinite one-dimensional porous medium, wavelike in form, with the steam and water zone behind it and the equilibrium zone in front of it. It is further assumed that all relevant variables defined over this one-dimensional infinite medium, such as the liquid saturation and the vapor concentration of the hydrocarbon, are everywhere continuous and almost everywhere differentiable, the exception being at the

distillation front where we admit jumps in spatial derivatives. Such jumps are required in order that both upstream and downstream conditions may be simultaneously satisfied. Given these continuity and differentiability assumptions, differential equations governing energy and mass balances, as well as those governing fluid flow, may be defined for the regions behind and ahead of the distillation front.

The governing equations

In Stokes flow, the mass flux of each continuous phase is directly related to the pressure gradients. The application of Darcy's law, modified for two-phase flow, including the effects of gravity forces and capillary forces, yields the following equations:

$$m_v = -\frac{\rho_v k k_{rv}}{\mu_v}\left(\frac{\partial p_v}{\partial x} + \rho_v g \sin\alpha\right), \quad (1)$$

and

$$m_w = -\frac{\rho_w k k_{rw}}{\mu_w}\left(\frac{\partial p_w}{\partial x} + \rho_w g \sin\alpha\right). \quad (2)$$

Introducing the capillary pressure, $p_c(s_w) = p_v - p_w$, and eliminating the pressure gradients in equations (1) and (2) gives the following fractional flow equation:

$$\frac{m_v}{\rho_v} f_1(s_w) - \frac{m_w}{\rho_w}[1 - f_1(s_w)] + \frac{k}{\mu_v} f_2(s_w)\left[p_c' \frac{\partial s_w}{\partial x} - (\rho_w - \rho_v) g \sin\alpha\right] = 0, \quad (3)$$

where $f_1(s_w)$, $f_2(s_w)$ and $p_c'(s_w)$ are functions of the water saturation defined in the following manner:

$$f_1(s_w) = \left[1 + \frac{\mu_w k_{rv}}{\mu_v k_{rw}}\right]^{-1}, \quad f_2(s_w) = k_{rv} f_1(s_w),$$

and

$$p_c' = \frac{dp_c}{ds_w}.$$

In the above equations, the capillary pressure, p_c, can be related to the water saturation through the following equation [19]:

$$p_c(s_w) = p_v - p_w = \sigma_{vw} J(s_w)\sqrt{\frac{\phi}{k}},$$

where σ_{vw} is the surface tension between the vapor phase and the water phase, and $J(s_w)$ is referred to as the Leverett function of capillarity. The particular functional form of $J(s_w)$ for a given porous material and fluids system can be determined experimentally.

At the interface of the liquid hydrocarbon and the gas in any pore, the hydrocarbon concentration in the vapor mixture can be assumed to be at the saturation concentration, c_s, i.e. the equilibrium concentration. In this work, we define the concentration as the mass of hydrocarbon vapor per total mass of the gas mixture. If an undersaturated vapor mixture exists in a nearby region, there would be a net mass flux from the liquid hydrocarbon phase to the vapor phase. The mass flux of hydrocarbon vapor into the vapor phase is assumed to be proportional to the difference between the equilibrium concentration and the undersaturated concentration away from the interface. Consider this mass transfer over a unit volume of the porous medium, in which there are numerous vapor–liquid hydrocarbon interfaces. By summing the mass fluxes at all these interfaces within a unit volume, we obtain the rate of evaporation of the liquid hydrocarbon, defined as the total mass of the liquid hydrocarbon converted to the vapor phase in a unit volume of porous medium per unit time. The volumetric rate of evaporation is then proportional to the difference between the equilibrium concentration and the local average concentration in the vapor mixture, c. The proportionality between the rate of evaporation and the concentration difference is referred to as the volumetric mass transfer coefficient, g_m. Through the use of the volumetric mass transfer coefficient, the (immobile) hydrocarbon liquid mass balance can be written as:

$$-\phi\frac{\partial(\rho_l s_l)}{\partial t} = g_m(c_s - c). \quad (4)$$

In general, g_m depends on the velocity of the vapor mixture, the liquid hydrocarbon and water saturations, the distribution of the phases, and the flow pattern of the vapor. It is broadly defined as the total amount of the mass of the hydrocarbon moving from liquid phase into vapor phase within a unit bulk volume of the porous medium per unit time due to a unit concentration difference in the vapor phase. The dimensions of g_m are $M\,L^{-3}\,T^{-1}$.

Mass and energy balance must also be considered in the formulation of the problem. The low temperature gradient and high flow rate of steam in the steam zone indicate that the contribution of convection is dominant in both mass and heat transfer. Neglecting dispersion and diffusion, we obtain the following species equation for steam and water:

$$\frac{\partial}{\partial x}[m_v(1-c) + m_w] + \phi\frac{\partial}{\partial t}[\rho_v s_v(1-c) + \rho_w s_w] = 0. \quad (5)$$

The conservation of mass of the hydrocarbon yields:

$$\frac{\partial}{\partial x}[m_v c] + \phi\frac{\partial}{\partial t}[\rho_v s_v c + \rho_l s_l] = 0. \quad (6)$$

By neglecting heat conduction, the following equation of conservation of energy can be written:

$$\frac{\partial}{\partial x}[h_s m_v(1-c) + h_v m_v c + h_w m_w] + \phi\frac{\partial}{\partial t}[e_v \rho_v s_v c + e_s \rho_v s_v(1-c) + e_l \rho_l s_l + e_w \rho_w s_w] = 0. \quad (7)$$

Thus, five equations, i.e. equations (3)–(7), for five unknown variables, s_w, s_l, c, m_v and m_w, are specified. The density of the liquid hydrocarbon and that of water can be assumed to be constant, while the density of the vapor mixture is a function of the concentration, temperature and pressure. By using specified, constant values of temperature and pressure in an appropriate equation of state, the density of the vapor mixture becomes a single-valued function of the hydrocarbon concentration. We note that equations (3)–(7) are first order in time and space, and thus, are hyperbolic in nature resulting in propagating wave solutions.

Upstream conditions

Since there is no liquid hydrocarbon present far upstream, boundary conditions there on hydrocarbon saturation and vapor concentration are:

$$c(-\infty, t) = 0, \quad s_l(-\infty, t) = 0. \tag{8}$$

In addition, the steam is injected at constant mass flow rate m_{in}, and constant quality X, yielding:

$$m_v(-\infty, t) = m_{in}X, \quad m_w(-\infty, t) = m_{in}(1-X). \tag{9}$$

It can be shown that the constant upstream vapor mass flux and water mass flux expressed by equation (9) result in constant upstream water saturation [12, 20]. By substituting equation (9) into the fractional equation (3) and applying the condition of a zero water saturation gradient, the constant upstream water saturation is obtained. Therefore, the fifth upstream boundary condition is:

$$s_w(-\infty, t) = s_{w-\infty}. \tag{10}$$

Downstream conditions

Assume that the value of the residual saturation of the liquid hydrocarbon directly behind the steam condensation front is known and the concentration of hydrocarbon in the vapor phase just behind the front is at the saturation concentration. Since we have assumed the steam condensation front to be far downstream, the following two downstream conditions then apply to the steam zone:

$$c(\infty, t) = c_s, \quad s_l(\infty, t) = s_{l\infty}. \tag{11}$$

If attention is focused on the region far enough behind the steam condensation front and far enough ahead of the distillation zone where the capillary driven flow is negligible, the mass flux of the vapor mixture, the mass flux of water, and the water saturation can be assumed to be constant. Thus,

$$m_v(\infty, t) = \text{constant}, \quad m_w(\infty, t) = \text{constant},$$
$$s_w(\infty, t) = \text{constant}. \tag{12}$$

SIMILARITY SOLUTION

Equations (3)–(7) are a system of hyperbolic first order partial differential equations defined on two spatial domains, one upstream and the other downstream of the distillation front. Jumps in spatial derivatives are allowed at the distillation front, thus 'weak' solutions to equations (3)–(7) may be found given the upstream and downstream conditions specified above. In the present problem, we assume that the spatial distributions (or waveforms) of the solution variables remain unaltered in shape and propagate (or translate) downstream all with the same (constant) velocity which happens to be that of the distillation front. This requires that any dependent solution variable, such as the hydrocarbon saturation, would have the functional from $s_l(x, t) = s_l(\eta)$, where,

$$\eta = x - v_c t. \tag{13}$$

We assume that the distillation front is located at $\eta = 0$, and the regions upstream and downstream of the front are $\eta < 0$ and $\eta > 0$, respectively. Matching the downstream conditions will implicitly specify the jumps in the derivatives at the distillation front; moreover, it is worth noting that the problem would be overspecified and therefore ill-posed if both downstream and jump conditions were specified. In addition, the assumption that the spatial distributions remain unaltered in shape and translate with the distillation front velocity is enough to specify the initial conditions when time is set to zero in equation (13). Using equation (13), equations (3)–(7) can be transformed to the following set of ordinary differential equations:

$$\frac{m_v}{\rho_v} f_1(s_w) - \frac{m_w}{\rho_w}[1 - f_1(s_w)] + \frac{k}{\mu_v} f_2(s_w)\left[p_c' \frac{ds_w}{d\eta} - (\rho_w - \rho_v) g \sin\alpha\right] = 0, \tag{14}$$

$$v_c \phi \frac{d(\rho_l s_l)}{d\eta} = g_m(c_s - c), \tag{15}$$

$$\frac{d}{d\eta}[m_v(1-c) + m_w - v_c \phi \rho_v s_v (1-c) - v_c \phi \rho_w s_w] = 0, \tag{16}$$

$$\frac{d}{d\eta}[m_v c - v_c \phi \rho_v s_v c - v_v \phi \rho_l s_l] = 0, \tag{17}$$

and

$$\frac{d}{d\eta}\{h_s m_v(1-c) + h_v m_v c + h_w m_w - v_c \phi[e_v \rho_v s_v c + e_s \rho_v s_v (1-c) + e_l \rho_l s_l + e_w \rho_w s_w]\} = 0. \tag{18}$$

The upstream boundary conditions are transformed to those for $\eta \to -\infty$ while the downstream conditions correspond to the conditions for $\eta \to \infty$. Therefore, all unknowns in the equations are functions of the only independent variable, η, which can be viewed as a coordinate attached to the distillation front and moving at velocity v_c with respect to the fixed coordinate, x.

Equations (16)–(18) can be integrated with respect

to η in the regions behind ($\eta < 0$) and ahead ($\eta > 0$) of the distillation front. The integration constants are then determined by evaluation of the resulting equations using the upstream and downstream boundary conditions. By continuity, the integrals of equations (16)–(18) are equal at the distillation front ($\eta = 0$), implying that the integration constants for the two regions, ($\eta < 0$) and ($\eta > 0$), are also equal. Equality of integration constants for equations (16)–(18), respectively, yields three algebraic equations in terms of four unknowns, v_c, $m_{v,}$, $m_{w,}$ and $s_{w,}$. During the process of eliminating $m_{v,}$ and $m_{w,}$, $s_{w,}$ is also fortuitously eliminated. Applying the basic relationships between the enthalpies and internal energies, we obtain the following equation for the characteristic velocity of the distillation zone:

$$v_c = \frac{m_{in} X}{\phi\left[\rho_s(1-s_{w-})+\rho_l s_{l\infty}\left(\frac{1}{c_s}+\frac{h_{vl}}{h_{sw}}-1\right)\right]}. \quad (19)$$

Equation (19) indicates that the characteristic velocity of the distillation zone is proportional to the mass flux of the injected steam. The velocity is also dependent on $s_{l\infty}$ and c_s such that for a high saturation of residual hydrocarbon or low equilibrium concentration, the velocity will be low, as expected. In the limit of $s_{l\infty} \to 0$, equation (19) gives an apparent distillation zone velocity equal to the vapor interstitial velocity. It is also notable that the velocity of the distillation zone decreases when the enthalpy of vaporization of the hydrocarbon is significant compared to that of water. This reduction is due to a condensation of the water vapor within the distillation zone as required to supply the energy for the hydrocarbon vaporization. As the water vapor mass flux decreases upon condensation, the mass flux of the hydrocarbon in the saturated vapor mixture leaving the distillation zone also decreases. Therefore, the velocity of the distillation zone must decrease.

Since the integration constants for the two regions, ($\eta < 0$) and ($\eta > 0$), are equal, we can evaluate the integration constants for the integrals of equations (16)–(18) in the region ahead ($\eta > 0$) of the distillation front using the upstream, as opposed to the downstream, boundary conditions. Having done so, these integrals form, for any specified value of η, a set of three algebraic equations in six unknowns, v_c, c, m_v, m_w, s_l and s_w. Elimination of m_v, m_w and s_w yields an expression for v_c which is similar to that in equation (19) except that liquid saturation, s_l, and concentration, c, appear rather than $s_{l\infty}$ and c_s. Equating this equation to equation (19) yields the following relationship between s_l and c:

$$c = \left[\frac{s_{l\infty}}{s_l c_s} + \left(\frac{s_{l\infty}}{s_l} - 1\right)\left(\frac{h_{vl}}{h_{sw}} - 1\right)\right]^{-1}, \quad \eta \geq 0. \quad (20)$$

Substituting equations (19) and (20) into this same set of three algebraic equations for the six unknowns, v_c, c, m_v, m_w, s_l and s_w, we can express m_v and m_w in terms of s_l and s_w. Taking these expression for m_v and m_w, together with equations (19) and (20), we can rearrange equations (14) and (15) into two coupled ordinary differential equations for the two unknowns, s_l and s_w. Since the upstream values of s_l and s_w are known and assumed constant for $\eta < 0$, and the solution is continuous at $\eta = 0$, we can integrate these two first order ordinary equations with any applicable method in the region, $\eta > 0$. Here we use the fourth order Runge–Kutta method. Once $s_l(\eta)$ and $s_w(\eta)$ are obtained, we can calculate the concentration, c, from equation (20). The mass fluxes, m_v and m_w, are obtained by back substituting values of s_l and s_w into the algebraic expressions for m_v and m_w. The pressure profiles of both liquid phase and vapor phase can also be obtained by transforming equations (1) and (2) to the η coordinate and then integrating them based on the obtained functions for m_v and m_w. More detailed descriptions of these derivations can be found elsewhere [20].

NONDIMENSIONALIZATION

For the sake of generality, equations (14)–(18) are nondimensionalized through the definition of the following parameters:

$$\xi = \frac{g_{rf}\eta}{m_{in}X}, \quad (21)$$

$$v_{cd} = \frac{\phi\rho_s}{m_{in}X} v_c, \quad (22)$$

$$N_{mf} = \frac{(m_{in}X)^2\mu_s}{g_{rf}\sqrt{\phi k}\sigma_{sw}\rho_s}, \quad (23)$$

$$N_{gr} = \frac{(\rho_w - \rho_s)kg\sin\alpha\rho_s}{m_{in}X\mu_s}, \quad (24)$$

and

$$v_{vd} = \frac{\phi\rho_s}{m_{in}X} v_v, \quad (25)$$

$$g_{md} = g_m/g_{rf}. \quad (26)$$

The dimensionless length, ξ, is the dimensional length, η, divided by a length that scales with the distance required for the steam to reach equilibrium conditions. The dimensionless velocity of the distillation zone, v_{cd}, and that of the vapor phase, v_{vd}, are the corresponding dimensional velocities scaled by a characteristic pore-scale steam velocity. The dimensionless number N_{mf} is the ratio of the length of the distillation zone to the length of the zone of variable water saturation. The dimensionless number N_{gr} is the gravity number, which gives the ratio of the gravity forces to the vapor phase viscous forces. The dimensionless mass transfer coefficient, g_{md}, is scaled by a reference mass transfer coefficient, g_{rf}.

After m_v and m_w are eliminated from equation (14) as outlined in the previous section, equations (14) and (15) can now be expressed in the following dimensionless forms:

$$\frac{ds_w}{d\xi} = -\frac{N_{mf}}{J'(s_w)}\frac{\rho_s}{\rho_l}\left\{\frac{v_{cd}\mu_v}{f_2(s_w)\mu_s}\left[\frac{\rho_s}{\rho_w}(1-f_1(s_w))\right.\right.$$
$$\times\left(1-\frac{1}{v_{cd}X}+\left(\frac{\rho_w}{\rho_s}-1\right)s_{wi}+\frac{\rho_l s_l}{\rho_s}\left(\frac{1}{c}-1\right)\right)$$
$$\left.+\left(1-s_l+\frac{\rho_l s_l}{\rho_s c}\right)f_1(s_w)-s_w\right]-N_{gr}\left(\frac{\rho_w-\rho_v}{\rho_w-\rho_s}\right)\Bigg\}, \quad (27)$$

and

$$\frac{ds_l}{d\xi} = g_{md}\frac{\rho_s}{\rho_l}\left(\frac{c_s-c}{v_{cdl}}\right). \quad (28)$$

These two equations are readily integrated to give the distributions of the water and liquid hydrocarbon saturations.

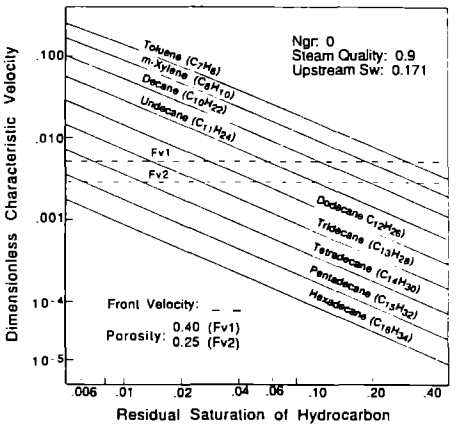

FIG. 2. Dimensionless distillation front velocity vs saturation of various hydrocarbons.

THEORETICAL RESULTS

The dimensionless velocities of the distillation zone as functions of the residual hydrocarbon saturation are shown in Fig. 2 for nine different compounds. The characteristic velocity of the distillation zone decreases with an increasing residual saturation of the compounds. For the same residual liquid saturation, the more volatile compounds have higher velocities. It is of note that in the limit of zero liquid saturation, the dimensionless distillation zone velocities shown in Fig. 2 must all converge to a value of $(1-s_{w-x})^{-1}$. Calculations also show that the gravity number, N_{gr}, affects the velocity only slightly and indirectly through the upstream saturation of water.

It is interesting to compare the characteristic velocities of the distillation zone with the velocity of the steam condensation front. Based on conservation of mass and conservation of energy, Stewart and Udell [12] derived the following relationship for the steam condensation front velocity:

$$\frac{\phi\rho_s v_f}{m_{in}X} = \frac{\rho_s}{\rho_w}\left[\frac{h_{sw}}{c_{pw}(T_f-T_i)}+\frac{1}{X}\right]\times\left[1-s_{l\infty}+\frac{(1-\phi)\rho_r c_{pr}}{\phi\rho_w c_{pw}}+\frac{\rho_s(1-s_{w-\infty})h_{sw}}{\rho_w c_{pw}(T_f-T_i)}-\frac{(\rho_l-\rho_s)}{\rho_w}(1-s_{w-x}-s_{l\infty})\right]^{-1}. \quad (29)$$

Dimensionless condensation front velocities for two example media are also plotted in Fig. 2 as the two dashed lines for different values of porosities (0.25 and 0.40) where the solid phase is assumed to be quartz ($\rho_r = 2.56\,\mathrm{g\,cm^{-3}}$ and $c_{pr} = 0.67\,\mathrm{kJ\,kg^{-1}\,°C^{-1}}$) and the temperature difference between the front and downstream ($T_f - T_i$) is 80°C. The condensation front velocity depends strongly on the porosity, the thermal properties of the solid phase, and the temperature downstream, while the characteristic velocity of the distillation zone is determined by thermodynamic constraints. These two velocities are independent of each other. If the condensation front velocity is greater than the characteristic velocity of the distillation zone, the distillation zone will lag behind. Otherwise, if the characteristic velocity of the distillation zone is greater than the condensation front velocity, the distillation zone will merge with the steam condensation front. For example, the characteristic velocity of toluene is larger than the condensation front velocity if the downstream saturation of the liquid toluene is less than 0.30 as shown in Fig. 2. Normally, after the viscous displacement by hot water ahead of the condensation front, we may expect that the residual saturation of liquid hydrocarbon in the steam zone will be below this level. Therefore, the steam would appear to completely displace the toluene at the steam condensation front even though the toluene has a higher boiling point than that of water. The nearly complete removal of toluene/benzene mixture by the steam front has been observed experimentally by Hunt *et al.* [7] and Stewart and Udell [12]. Similar observations were made during the steam displacement of xylene during other unpublished experiments. These observations are in agreement with the theoretical findings reported herein.

Equality of the steam condensation front and distillation zone velocities established an important division between the situation of hydrocarbon removal solely at the steam condensation front, and the situation where the distillation zone will lag behind the steam condensation front. If the velocity of condensation front is less than that of the distillation zone, the hydrocarbon liquid would evaporate only as rapidly as the steam can come into contact with it. Then the distillation zone velocity would be limited by the condensation front velocity. This condition is termed frontal removal. A separate distillation zone will exist only if the velocity of the condensation front is higher than the velocity of the distillation zone. By

assuming that the ideal gas law applies, the saturated concentration c_s in equation (19) can be expressed in terms of the saturation pressures and molecular weights of the compound and water. Equating the dimensionless characteristic velocity of the distillation zone to the dimensionless steam condensation front velocity, v_{fd} (defined by equation (29)), we obtain the following criterion for frontal removal:

$$\rho_l s_{lr} \leqslant \frac{\rho_s\left[\frac{1}{v_{fd}} - (1 - s_{w\ r})\right]}{\frac{p_s M_w}{p_o M_o} + \frac{h_{vl}}{h_{sw}}}. \qquad (30)$$

Equation (30) is plotted in Fig. 3 using average values of the latent heat of vaporization of various hydrocarbon compounds listed in Fig. 2. The region beneath the corresponding curve in Fig. 3 represents conditions where the liquid compounds are vaporized at the steam condensation front, whereas the region above represents conditions allowing a separate, slower moving distillation zone.

In order for the distributions of the concentrations, liquid saturations, and phase pressure distributions to be calculated, the dimensionless mass transfer coefficient, g_{md}, must be defined. However, the volumetric mass transfer coefficient defined in equation (4) is a difficult parameter to evaluate. Microscopically, evaporation of liquid hydrocarbon takes place at the interface between the liquid hydrocarbon and the vapor phase. We may expect intuitively that the mass transfer coefficient is an increasing function of the velocity of the vapor phase, the saturation of the liquid hydrocarbon, the vapor pressure, and the diffusivity of the hydrocarbon vapor in the steam. This parameter will also be strongly affected by the pore structure of the medium and configuration of the immobile hydrocarbon ganglia. If the hydrocarbon liquid is dispersed as droplets inside the pores, the amount of the liquid hydrocarbon evaporated in a unit bulk volume of the porous medium will be proportional to the number of the liquid drops in the volume which, in turn, is proportional to the saturation of the liquid hydrocarbon. Thus, in an average sense, one might postulate that the mass transfer coefficient will be proportional to the saturation of liquid hydrocarbon. On the multiple pore scale, the mass transfer processes are governed diffusion across a concentration boundary layer in which the Sherwood number is proportional to the square root of the superficial velocity [7]. Thus, for the purpose of example calculations, the dimensionless mass transfer coefficient is assumed to be equal to the liquid saturation multiplied by the square root of the dimensionless velocity of the vapor phase:

$$g_{md} = s_l v_{vd}^{0.5}. \qquad (31)$$

For all calculations, the following relationships for relative permeabilities and capillary pressures are used:

$$krw(sw) = s^3, \quad krv(sw) = (1-s)^3 \quad \text{and}$$

$$J(sw) = 1/\sqrt{s} - 1$$

where

$$s = \frac{s_w - s_{w,irr}}{1 - s_{lr} - s_{w,irr}},$$

The irreducible water saturation, $s_{w,irr}$, is defined as the water saturation below where there is no hydraulic connectivity, and thus would not flow under an applied pressure gradient.

Results of example calculations using decane as the organic compound are shown in Figs. 4–7. Profiles of

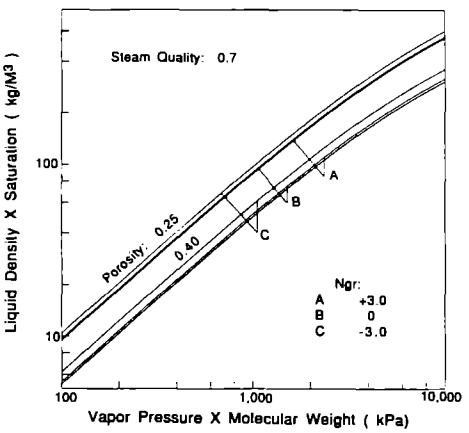

FIG. 3. Maximum quantity of residual hydrocarbon that can be removed directly behind the steam condensation front.

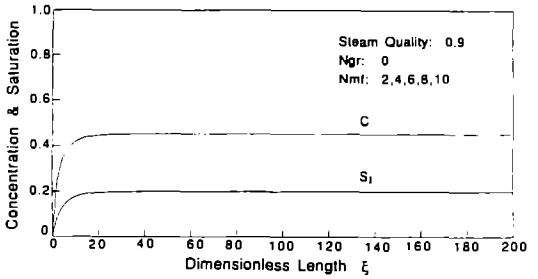

FIG. 4. Vapor concentration and liquid saturation profiles for decane.

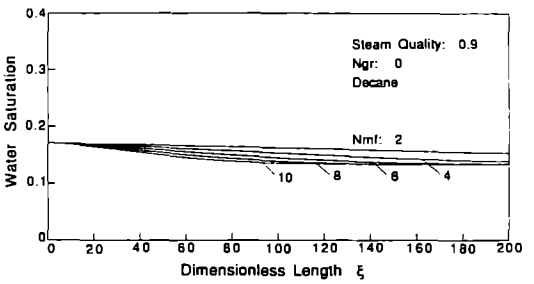

FIG. 5. Water saturation profiles for various dimensionless numbers, N_{mf}.

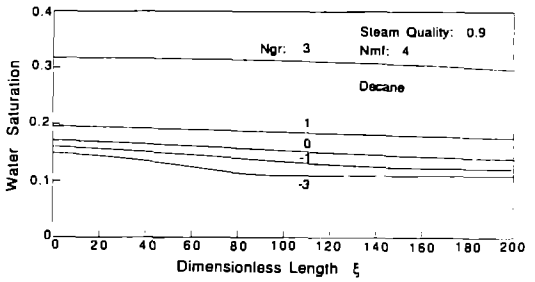

FIG. 6. Water saturation profiles for various gravity numbers.

the vapor hydrocarbon concentration and saturation of liquid decane (Fig. 4), the water saturation (Figs. 5 and 6), and the pressure gradients of both the vapor phase and the water phases (Fig. 7) are plotted against the dimensionless length. The values of other parameters, including dimensionless numbers $N_{\rm fm}$ and $N_{\rm gr}$ and the quality of injected steam are shown in the figure legends and captions. Figure 4 presents the vapor concentration and liquid saturation of dodecane vs dimensionless length ξ. As shown, there is no perceivable effect of the dimensionless numbers $N_{\rm fm}$ and $N_{\rm gr}$ on the distributions of the vapor concentration and the liquid saturation of the compound. This apparent independence is no surprise since these parameters do not explicitly appear in equations (15) and (20). They affect the concentration profile only through the vapor velocity, $v_{\rm vd}$, which determines the dimensionless mass transfer coefficient, $g_{\rm md}$, in equation (15). But the dimensionless vapor velocity itself is nearly constant because of the limited changes in the density of the vapor phase. Note also that the major change in the concentration and the liquid saturation occurs near $\xi = 0$. This range of ξ may be referred to as the mass-transfer-controlled region and is determined by the initial saturation of the liquid phase and the thermodynamic properties of the compound through equations (15) and (20). Thus the actual length of the medium for the mass-transfer-controlled region is proportional to the mass flux of injected steam $m_{\rm in}X$ and inversely proportional to the mass transfer coefficient $g_{\rm rf}$.

Water saturations vs the dimensionless length, ξ, are plotted in Figs. 5 and 6 for various combinations of

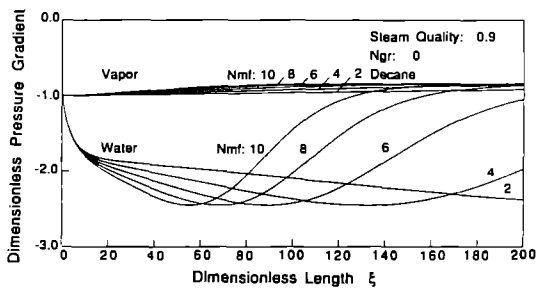

FIG. 7. Profiles of the dimensionless pressure gradients of the vapor and water phases.

$N_{\rm mf}$ and $N_{\rm gr}$ as indicated in each plot. As previously discussed, the upstream water saturation is determined by the quality of injected stream and is employed as one of the boundary conditions for equations (27) and (28). The downstream water saturations obtained from integration in each plot converge to a constant value determined by the downstream flow conditions. From both Figs. 5 and 6 we find that the water saturation decreases with ξ. The reason for this is that the characteristic velocity of the distillation zone is much higher than the interstitial velocity of the water phase, but much lower than the velocity of the vapor phase. When we observe the distillation zone from a moving coordinate associated with η or ξ, we see that as the vapor is flowing by, part of the steam condenses to the liquid water which would appear to be flowing upstream. Thus, the profile of water saturation in the ξ coordinate appears as a decreasing function. The particular form of the water saturation profile depends on the functional forms for the relative permeabilities and capillarity pressure.

Figure 5 shows that the parameter $N_{\rm mf}$ has no effect on the downstream water saturation. It merely changes the transition length of water saturation compared to the length of the mass-controlled region. The saturation of water decreases from a constant upstream value to a constant downstream value. The higher the injection rates, corresponding to greater values of $N_{\rm mf}$, the shorter the transition zones of the water saturation.

Figure 6 shows the effects of $N_{\rm gr}$ on the water saturation profiles when $N_{\rm mf}$ is a constant. The effects of $N_{\rm gr}$ on water saturation can be discussed through the dip angle of the medium. When the dip angle increases and $N_{\rm gr}$ is greater than 1, the water saturation must increase to overcome the unfavorable gravity force effect and to maintain the same water flux. Therefore, increasing the value of $N_{\rm gr}$ results in higher water saturation for the whole distillation zone and longer transition region for water saturation.

Figure 7 shows the dimensionless pressure gradients of the vapor and water phases. The upstream pressure gradients of both phases are identical and are used to nondimensionalize the pressure gradients. The behavior of these pressure gradients is found to be consistent with the water saturation distributions. The absolute value of the dimensionless pressure gradient of the vapor phase is very close to one. Thus, vapor pressure gradients are nearly constant in the steam zone and in agreement with experimental observations [12].

EXPERIMENTAL RESULTS

A one-dimensional experiment of steam distillation of dodecane was performed for model comparison and to obtain the actual mass transfer coefficient as a function of the liquid hydrocarbon saturation. A

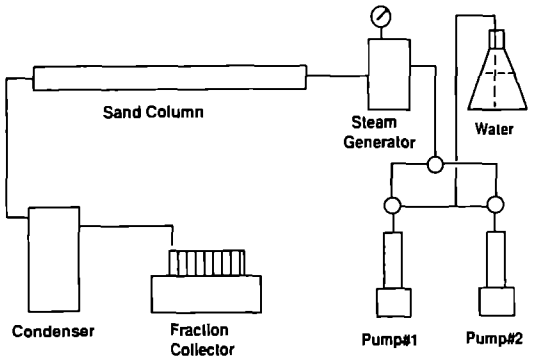

FIG. 8. Schematic drawing of experimental apparatus.

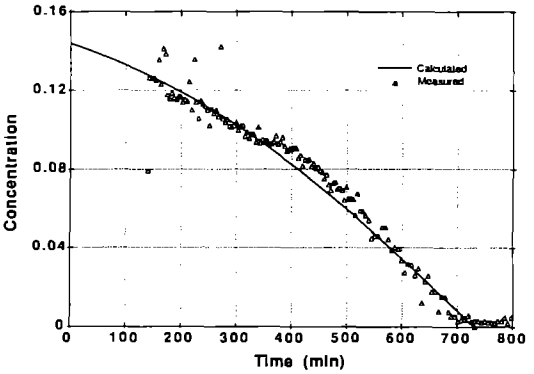

FIG. 10. Dodecane concentration in the vapor phase as measured in the effluent.

schematic of the apparatus used is shown in Fig. 8, in which the sand pack, consisting of a glass tube 1 m in length and 5.08 cm in ID, was packed with 100–115 mesh Ottawa sands. A total amount of 223 g of liquid dodecane was injected into the sand pack when it was initially saturated with air. The corresponding liquid saturation of dodecane was 0.404. Then deionized and deaerated water was injected at room temperature to displace the liquid dodecane. After about 6 pore volumes of fluid was produced, water injection was stopped. At that moment, the volumetric fraction of liquid dodecane in the effluence decreased to the level of 1×10^{-3}. The average saturation of liquid dodecane in the sand pack was calculated to be 0.174. Then steam was injected into the sand pack. The effluent of condensed water and liquid dodecane was collected by a fraction collector, which collected liquid samples into individual test tubes at equal time intervals. The liquid dodecane and water in each test tube were separated and weighed. Based on these data, the cumulative production history of water and dodecane was obtained and plotted in Fig. 9. As shown in Fig. 9, before steam breakthrough the slope of the cumulative water production curve was lower after steam breakthrough because the water displacement by steam no longer was important. Before steam breakthrough, almost no liquid dodecane was produced, which supports the assumption of liquid hydrocarbon at a residual level prior to steam injection. After steam breakthrough, the cumulative production of dodecane increases and finally approaches a constant when no more dodecane appeared in the condensed effluent. Letting the moment of steam breakthrough be the beginning time, we may define the cumulative water production function, $V_w(t)$, and the dodecane cumulative production function, $V_l(t)$, by regression methods. Neglecting the liquid water flux from the column after steam breakthrough, the concentration of dodecane in the vapor at the end of the sand pack can be obtained from the following equation:

$$c(t) = \frac{V_l'(t)\rho_l}{V_w'(t)\rho_w + V_l'(t)\rho_l}, \tag{32}$$

where the prime on the functions V_l and V_w indicates their time derivatives. From equation (20) the liquid saturation of dodecane can be expressed in terms of the corresponding concentration:

$$s_l(t) = \frac{s_{lr}\left(\frac{1}{c_s} + \frac{h_{vl}}{h_{sw}} - 1\right)}{\frac{1}{c(t)} + \frac{h_{vl}}{h_{sw}} - 1}. \tag{33}$$

Then from equation (4), the mass transfer coefficient g_m can be expressed as:

$$g_m(t) = -\frac{\phi\rho_l}{c_s - c(t)}\frac{ds_l}{dt}. \tag{34}$$

Substituting (32) and (33) into (34), we obtain the mass transfer coefficient at the end of the sand pack as a function of time. Correlating $g_m(t)$ with the liquid saturation $s_l(t)$ using linear regression methods, we obtain the following correlation between mass transfer coefficient and the liquid saturation:

$$g_m = 5.82 \times 10^{-3} + 6.08 \times 10^{-2} \times s_l. \tag{35}$$

By letting the reference mass transfer coefficient g_{rf} be 1 km m^{-3} s^{-1}, the dimensionless mass transfer coefficient g_{md} as a function of the liquid saturation is that from equation (34). Employing equation (35) instead of equation (31) and performing simultaneous integration of equations (27) and (28), we get the concentration in the vapor phase at the end of the sand pack. Figure 10 shows that the calculated con-

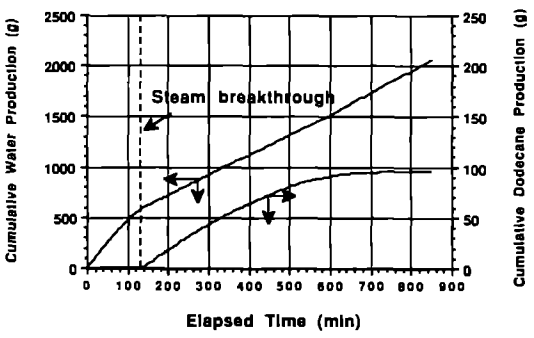

FIG. 9. Cumulative production of water and dodecane.

centrations compared to the measured data. Since the mass transfer coefficient given by equation (35) was obtained from the effluent concentration data, the close correlation between theory and data is expected. For this particular experiment the calculated distillation zone velocity equaled 6.17×10^{-5} m s^{-1} and the length of the distillation zone was 5.32 m.

CONCLUSIONS

The following conclusions can be drawn from the theoretical and experimental investigation of steam distillation of a single component hydrocarbon liquid in a one-dimensional porous medium.

(1) Given certain side conditions, similarity solutions can be found for the one-dimensional single component steam distillation problem if diffusion in the flow direction is neglected.

(2) The characteristic velocity of the distillation zone is proportional to the mass flux of the injected steam. The proportionality coefficient is a function of the water saturation far downstream of the liquid compound, the equilibrium concentration of the compound in the vapor phase, and the ratio of the latent heat of the liquid compound to that of the water. For distillation zone velocities greater than the steam condensation front velocity, the liquid compound is expected to be vaporized directly behind the steam condensation front.

(3) The lengths of the active mass transfer zone are proportional to the mass flux of the injected steam and inversely proportional to the mass transfer coefficient. The gravity and capillary forces have little effect on this length.

(4) Relative to the moving distillation zone, the water saturation appears as a decreasing function in the flow direction because the velocity of condensed water is less than the velocity of the distillation front. The length of the variable water saturation transition zone is significantly affected by the gravity number, and the length of the variable water saturation zone compared to the length of the distillation zone varies as a function of a second dimensionless parameter, N_{fm}.

(5) A volumetric mass transfer coefficient that varies in a linear fashion with the liquid hydrocarbon saturation is representative of the experiments conducted for this study.

Acknowledgements—The authors wish to acknowledge the financial support provided by the U.S. Environmental Protection Agency, grant No. R-815247-01-0, and the National Institute of Environmental Health Sciences, grant No. 3 P42ES04705-0251. The assistance of Alan R. Crockett in the review of the formulation of the theoretical model is also acknowledged.

REFERENCES

1. S. L. Stovall, Recovery of oil from depleted sands by means of dry steam, *Oil Weekly*, 17–24 (13 August 1934).
2. C. W. Volek and J. A. Pryor, Steam distillation drive, Brea Field, California, *J. Pet. Tech.* 899–906 (1972).
3. A. L. Hall and R. W. Bowman, Operation and performance of a Slocom thermal recovery project, *J. Pet. Tech.* 402–408 (1973).
4. R. H. Widmyer *et al.*, The Charco Redondo thermal recovery pilot, *J. Pet. Tech.* 1522–1532 (1977).
5. SPE Field Report, *Enhanced Oil Recovery Field Reports*, Vol. 8, No. 1, pp. 685–686, SPE, Richardson Texas (1982).
6. T. R. Blevins, J. H. Duerksen and J. W. Ault, Light-oil steamflooding—an emerging technology, *J. Pet. Tech.* 1115–1122 (1984).
7. J. R. Hunt, N. Sitar and K. S. Udell, Nonaqueous phase liquid transport and cleanup, *Water Resources Research* **24,** 1247–1269 (1988).
8. B. Hilberts, *In-situ* steam stripping, *Proceedings of First International TNO Conference on Contaminated Soil* (Edited by J. W. Assink and W. J. van den Brink), pp. 680–687, Utrecht, The Netherlands, 11–15 November (1985).
9. K. S. Udell and L. D. Stewart, Mechanisms of *in-situ* remediation of soil and groundwater contamination by combined steam injection and vacuum extraction, *Proceedings of Conference on Subsurface Contamination by Immiscible Fluids*, Calgary, Canada, April (1990).
10. B. T. Willman, V. V. Valleroy, G. W. Runberg, A. J. Cornelius and L. W. Powers, Laboratory studies of oil recovery by steam injection, *J. Pet. Tech.* 681–690 (July 1961).
11. C. H. Wu, A critical review of steamflood mechanisms, Paper SPE 6650 *Proceedings of the 1977 SPE California Regional Meeting*, Bakersfield, April (1977).
12. L. D. Stewart and K. S. Udell, Mechanisms of residual oil displacement by steam injection, *SPE Reservoir Engineering*, pp. 1233–1242, November (1988).
13. S. M. Farouq Ali, Jr., Practical considerations in steamflooding, *Producers Monthly*, 13–16 (January 1968).
14. F. S. Johnson, C. J. Walker and A. F. Bayazeed, Oil vaporization during steamflooding, *J. Pet. Tech.* 731–742 (June 1971).
15. C. H. Wu and A. Brown, Laboratory study on steam distillation in porous media, Paper SPE 5569, *SPE Annual Technical Conference*, Dallas, 28 September–1 October (1975).
16. C. H. Wu and R. B. Elder, Correlation of crude oil steam distillation yields with basic crude oil properties, *Soc. Pet. Eng. J.* 937–945 (December 1983).
17. J. H. Duerksen and L. Hsueh, Steam distillation of crude oils, *Soc. Pet. Eng. J.* 265–271 (April 1983).
18. D. K. Menegus and K. S. Udell, A study of steam injection into water saturated capillary porous media, *Heat Transfer in Porous Media and Particulate Flows*, Vol. 46. ASME Heat Transfer Div., New York (1985).
19. M. C. Leverett, Capillary behavior in porous solids, *AIME Trans.* **142,** 152–169 (1941).
20. Zeng G. Yuan, Steam distillation of liquid hydrocarbon mixtures in porous media, Ph.D. thesis, University of California, Berkeley, California (1990).